

Mechanical design of ultraprecision weak-link stages for nanometer-scale x-ray imaging

This article has been downloaded from IOPscience. Please scroll down to see the full text article.

2009 J. Phys.: Conf. Ser. 186 012017

(<http://iopscience.iop.org/1742-6596/186/1/012017>)

View [the table of contents for this issue](#), or go to the [journal homepage](#) for more

Download details:

IP Address: 38.107.191.117

The article was downloaded on 09/09/2010 at 11:35

Please note that [terms and conditions apply](#).

Mechanical design of ultraprecision weak-link stages for nanometer-scale x-ray imaging

D. Shu¹ and J. Maser^{2,3}

¹APS Engineering Support Division, Argonne National Laboratory, Argonne, IL 60439, USA

²Center for Nanoscale Materials, Argonne National Laboratory, Argonne, IL 60439, USA

³X-ray Sciences Division, Argonne National Laboratory, Argonne, IL 60439, USA

shu@aps.anl.gov

Abstract. A nanopositioning diagnostic setup has been built to support the Argonne Center for Nanoscale Materials (CNM) nanoprobe instrument commissioning process at the APS. Its laser Doppler interferometer system provides subnanometer positioning diagnostic resolution with large dynamic range. A set of original APS designed ultraprecision PZT-driven weak-link stages with high-stiffness motor-driven stages has been tested with this diagnostic setup.

In this paper we present a preliminary test result of the ultraprecision weak-link stage system developed for the CNM hard x-ray nanoprobe instrument at APS sector 26. A test result for a novel laminar weak-link mechanism with sub-centimeter travel range and sub-nanometer positioning resolution is also introduced in this paper as a future work.

1. Introduction

The CNM hard x-ray nanoprobe instrument at APS sector 26 combines a scanning probe mode with a full-field transmission mode. It uses x-ray fluorescence for trace element mapping and spectroscopy; x-ray diffraction to obtain local structural information such as crystallographic phase, strain texture, and x-ray transmission in phase; and absorption to image internal structures of complex devices [1]. The nanoprobe instrument is designed for operating with photon energies between 3 keV and 30 keV with 30-nm spatial resolution. Imaging and spectroscopy at this resolution level require staging of x-ray optics and specimens with a mechanical repeatability of better than 10 nm [1].

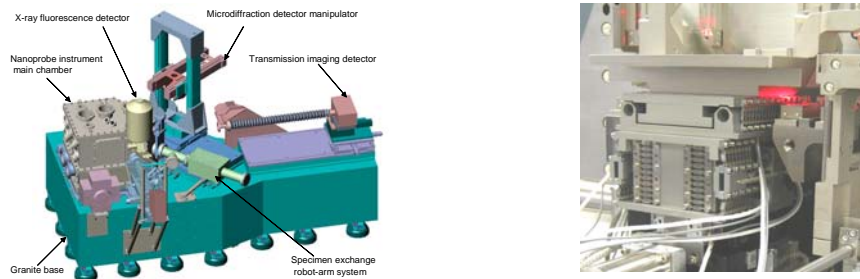


Fig. 1. Left, a 3-D model of the the optomechanical structure for the hard x-ray nanoprobe instrument. Right, photograph of the ultraprecision weak-link stage system for FOM.

As shown in Figure 1 (left side), the optomechanical structure for the CNM hard x-ray nanoprobe instrument consists of the following major subassemblies: a granite base, a nanoprobe instrument main

chamber with scanning stages for x-ray focusing optics and sample stages, an industrial robot-arm-based microdiffraction detector manipulator, a stage system for an x-ray transmission imaging detector, a stage system for an x-ray fluorescence detector, and a precision specimen exchange robot-arm system to provide automated high-throughput operation capability [2]. Inside the instrument main chamber, the positioning stages for the optics are grouped into several subcomponents that are engineered to move in or out of the beam to allow configuration of the instrument for scanning probe mode and full-field transmission mode. Fast feedback for differential vibration control between the zone-plate x-ray optics and the sample holder has been implemented in this design. A specially designed, custom-built laser Doppler displacement meter (LDDM) system provides two-dimensional differential displacement measurement with subnanometer resolution between the focusing optics module (FOM) and the specimen module (SM) [3].

2. Linear stages with laminar overconstrained weak-link mechanisms

Unlike traditional kinematic flexure mechanisms, laminar overconstrained weak-link mechanisms provide much higher structure stiffness and stability. Using photochemical machining processes with lithography techniques we are able to construct a strain-limited overconstrained mechanism on the thin metal sheets. By stacking these thin-metal weak-link sheets with alignment-pins, we can construct a solid complex laminar weak-link structure with ultrahigh positioning sensitivity and stability [4-6]. More than forty sets of rotary laminar weak-link mechanisms have been made for APS users in synchrotron radiation instrumentation applications, such as high-energy-resolution monochromators for inelastic x-ray scattering, and x-ray analyzers for ultra-small-angle scattering and powder-diffraction experiments. Linear laminar weak-link mechanisms also demonstrated high resolution with high-stiffness for high-precision linear stage applications, such as x-ray microscopy applications.

Figure 1 (right side) shows the stages for the nanoprobe FOM manufactured by Xradia, Inc. [7], which provide a three-dimensional positioning capability with 0.125-nm LDDM measuring resolution in 12 mm x 12 mm x 12 mm range. It includes three stepping-motor-driven translation stages and two PZT-driven high-stiffness stages using overconstrained weak-link parallelogram mechanisms for ultraprecision motion control.

As shown in Figure 2 (left side), two PZT drivers are applied for the horizontal PZT-driven stage (APS T8-22) to guarantee the linear motion trajectory accuracy in a specific direction. The resolution of the stage is 0.2-nm with a travel range of 15 microns. To gain a higher positioning resolution, two sets of precision motion reduction mechanisms using laminar weak-link structures are implemented in the APS PZT-driven vertical stage T8-23 as shown in Figure 2 (middle-left side). Each set of precision motion-reduction mechanism was driven by a pair of PZT actuators to provide a 0.05-nm positioning resolution in a 4-micron travel range with a 5-kg load capacity. Physik Instrumente PI-841.10 PZT actuators with E-509 strain gauge sensor servo-control modules [8] were used to drive both APS T8-22 and T8-23 weak-link stages.

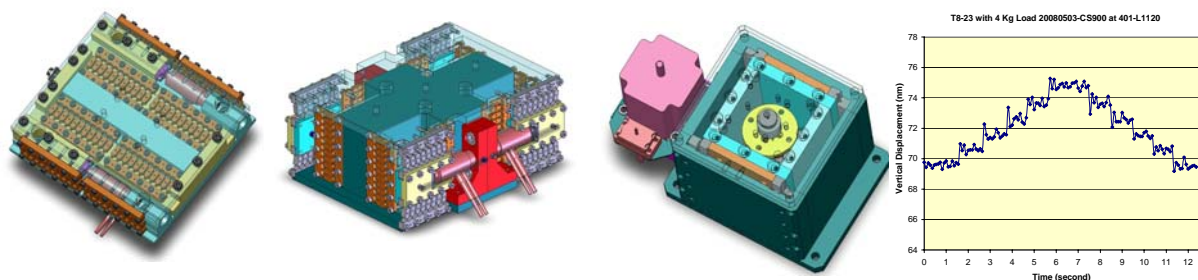


Fig. 2. Left, a 3-D model for the APS T8-22 PZT-driven horizontal stage. Middle-left, a 3-D model for the APS T8-23 PZT-driven vertical stage. Middle-right, a 3-D model for the APS T2-24 stepping-motor-driven vertical stage. Right, a series of 1-nm steps generated by the APS-designed T8-23 ultraprecision weak-link stage on top of the original T2-24 high-stiffness motor-driven stage with a 4-kg load under LDDM closed-loop control. The test is performed with a nanopositioning diagnostic setup on an optical table at the APS nanopositioning lab.

The structural stiffness of the stepping-motor-driven stage (APS T2-24), the base of two motorized horizontal stages and two PZT-driven stages, is critical to the final performance of the FOM stages group. Argonne has developed a special crossed roller linear guiding system with sub micron positioning sensitivity and 2-D heavy preloading capability. The coupling structure between the T2-24 guiding system and its driver's leading screw is also unique. As shown in Figure 2 (middle-right side), it can decouple any misalignment between the two motion components and ensure the positioning sensitivity and structural stiffness performances of both stages [9].

3. Test of the weak-link stages with the APS nan positioning diagnostic setup

Although the single horizontal weak-link stage has demonstrated Angstrom level positioning sensitivity and stability at the APS since 2002 [10], many construction and commissioning details needed to be optimized to ensure reliable nanometer-scale operation for a multi-dimensional scanning stage system with a few-kilogram load capacity for the CNM nanoprobe FOM.

A nan positioning diagnostic setup has been built to support the CNM nanoprobe instrument commissioning process at the APS. Its laser Doppler interferometer system provides subnanometer positioning diagnostic resolution with large dynamic range. A set of original APS-designed ultraprecision PZT-driven weak-link stages T8-22 and T8-23 with a high-stiffness vertical motor-driven stage T2-24 has been tested with this diagnostic setup. A series of 1-nm steps generated by the APS T8-23 ultraprecision weak-link stage on top of the T2-24 vertical motorized stage with a 4-kg load under LDDM closed-loop control is demonstrated as shown in Figure 2 (right side). To support the CNM nanoprobe instrument commissioning process, more tests will be performed for motorized vertical stages with different construction and assembly conditions.

4. Future work for ultraprecision linear weak-link stages

For scanning microscope instrumentation developers it is always a dream to have a compact single stage to cover large travel range with very high positioning resolution. Based on an advanced structure design with a laminar overconstrained weak-link technique, we are exploring the feasibility of building a weak-link-based precision linear guiding system with sub-nanometer resolution and sub-centimeter travel range with a reasonably compact size [11]. A test stage for a single weak-link module has been constructed with sizes of 120 mm x 130 mm x 25 mm. A 3-mm travel range is demonstrated in this test with 3- to 4- μ rad tilt errors in the middle of 2.4 mm travel range. Using four such modules, a vertical weak-link stage has been designed for a scanning sample stage system for a hard x-ray test setup with multilayer Laue lenses (MLLs) [12].

Acknowledgments

The authors would like to thank D. Nocher and R. Ranay from Argonne National Laboratory for their help in the development of laminar weak-link mechanisms. This work was supported by the U.S. Department of Energy, Office of Science, Office of Basic Energy Sciences, under Contract No. DE-AC02-06CH11357.

References

- [1] J. Maser et al., Proc. 8th Int. Conf. X-ray Microscopy, IPAP Conf. Series 7 (July 2006) 26-29.
- [2] D. Shu et al., Proc. 8th Int. Conf. X-ray Microscopy, IPAP Conf. Series 7 (July 2006) 56-58.
- [3] U.S. Patent granted No. 7,331,714, D. Shu, J. Maser, B. Lai, F. S. Vogt, M. V. Holt, C. A. Preissner, R. Winarski, and G. B. Stephenson, 2008.
- [4] U.S. Patent granted No. 6,607,840, D. Shu, T. S. Toellner, and E. E. Alp, 2003.
- [5] U.S. Patent granted No. 6,984,335, D. Shu, T. S. Toellner, and E. E. Alp, 2006.
- [6] D. Shu, T. S. Toellner, and E. E. Alp, Nucl. Instrum. and Methods A 467-468 (2001) 771-774.
- [7] Xradia is a trademark of the Xradia Inc. California, U.S.A.
- [8] Physik Instrumente (PI) is a trademark of the Physik Instrumente GmbH & Co. Germany.
- [9] U.S. Patent granted No. 5,526,903, D. Shu, and J. Barraza, 1996.
- [10] D. Shu, Y. Han, T. S. Toellner, and E. E. Alp, Proc. SPIE Vol. 4771 (2002) 78-90.
- [11] D. Shu and J. Maser, U.S. Patent application in progress for ANL-IN-08-013.
- [12] J. Maser et al., Proc. SPIE-Int. Soc. Opt. Eng. 5539 (2004) 185.